10th International Symposium on Hydraulic Structures Zurich, Switzerland 17-19 June 2024
ISSN 0374-0056 DOI: 10.3929/ethz-b-000675997

Self-Aeration and Energy Dissipation on Concrete Gravity Dam Stepped Spillway: Hybrid Modelling Mark II

H. Chanson[1] & J. Hu[1]
[1]*The University of Queensland, School of Civil Engineering, Brisbane QLD 4072, Australia*
E-mail: h.chanson@uq.edu.au

Abstract: *For the last decades, a number of overflow stepped spillways were built because the staircase shape is conducive to reduced construction costs and increased rate of energy dissipation. Stepped spillways are characterised by highly turbulent air-water flows and a significantly larger rate of energy dissipation compared to smooth chutes. Herein, detailed measurements were performed in a large-size 1V:0.8H stepped spillway model and complemented with 1V:0.8H stepped spillway prototype data. The steep slope is typical of modern concrete gravity dams. The laboratory facility was a 15:1 scale model of the large dam's stepped spillway where field observations were conducted between 2013 and 2024. Froude similar experiments were conducted based upon the 2021 flood conditions and detailed two-phase flow measurements were undertaken to characterise finely the self-aeration and rate of energy dissipation. The hybrid modelling Mark II combined physical and field measurements and it delivered herein a composite approach yielding some robust estimates directly relevant to design engineers.*

Keywords: *Stepped spillways, Air-water flows, Concrete gravity dam spillways, Hybrid modelling Mark II, Energy dissipation.*

1. Introduction

During the last six decades, a number of dam spillways were built with a stepped profile because the staircase bywash shape is conducive to an increased rate of energy dissipation and reduced construction costs (Sorensen 1985, Chanson 1995). During operation, the stepped spillway flows are characterised by a highly turbulent motion and intense self-aeration together with a large rate of energy dissipation compared to smooth chutes (Chanson 2001, Boes and Hager 2003). In major floods, the energy dissipation rate may exceed the electrical outputs of large nuclear power plants (Chanson 2015). While stepped spillways have been built for several millennia, the advancements in concrete construction technology, including roller compacted concrete (RCC) and immersion vibrated roller compacted concrete (IVRCC), has led to a strong interest for the stepped spillway design with concrete gravity dams during the last 60 years (Fig. 1) (Matos and Meireles 2014). Figure 1 presents an overflow stepped spillway at a modern concrete gravity dam; note the small size of the downstream energy dissipator.

The hydraulic design of stepped spillways is fairly complicated owing to the hydrodynamic challenges, with several distinctive flow regimes, some intricate air-water fluid dynamics, and the huge amounts of energy dissipation above the steps (Chanson 1995,2001). The hydraulic modelling may be conducted physically, computationally, or in combination. All approaches have some limitations (Bombardelli 2012). Recent developments encompass two types of hybrid modelling: Mark I combining physical and CFD modelling, and Mark II with a complementary usage of laboratory data and field observations (Chanson 2022a). Although challenging, the latter has a potential to deliver accurate scientifically-based energy dissipation predictions and hence robust and reliable spillway design guidelines.

Field observations were conducted at the Hinze Dam stepped spillway (Australia) between 2013 and 2024 (Fig. 2). In complement, new physical measurements were conducted in a 15:1 three-dimensional physical model with Froude similar experimental flow conditions corresponding to 2021 major flood conditions. Detailed air-water flow measurements were undertaken to characterise the self-aeration and rate of energy dissipation. The physical results are discussed in comparison to some prototype observations of large flood flows at the Hinze Dam stepped spillway.

2. Study Site and Physical Modelling

The Hinze Dam is located on the Nerang River in the Gold Coast Hinterland, in eastern Australia. The present spillway comprises of a compound ogee crest followed by a 1V:0.8H steep stepped chute ending in an energy dissipator with baffle blocks (Phillips and Ridette 2007). The stepped chute is equipped with 1.5 m high 1.2 m long steps made of conventional concrete (Fig. 2). Its operation was extensively documented between 2013 and 2024 (Chanson 2022b).

Figure 1. Concrete gravity dam stepped spillway: Riou Dam (France) in 2004, h = 0.43 m, 1V:0.6H slope.

New physical experiments were performed in a stepped spillway physical model located at the University of Queensland (UQ). The laboratory chute was designed as a simplified three-dimensional 15:1 scale model of the Hinze Dam stepped spillway. The water was supplied by three adjustable altering currents (AC) pumps feeding a 1.7 m deep and 5 m wide concrete basin. The flow was smoothly converged into a symmetrical sidewall convergent before entering the 0.985 m wide test section (Fig. 3). The convergent ensured a smooth and waveless flow into the upstream broad-crested weir (Chaokitka and Chanson 2022). The crest controlled the flow over the 1.4 m high stepped chute, equipped with 0.10 m high and 0.08 m long steps made of smooth PVC.

The flow rate was deduced from the measured head above crest using a carefully-calibrated stage discharge relationship (Chaokitka and Chanson 2022). Clear-water flow depths were measured with a pointer gauge mounted over the channel centreline. The air-water flow measurements were performed using a two-tip phase-detection probe, designed, developed and manufactured at the University of Queensland. The probe was equipped with two identical needles ($\varnothing$ = 0.25 mm) separated by a streamwise distance Δx_{tip} = 9.0 mm. Each needle was sampled at 20 kHz for 45 s. The air-water flow properties were measured at several cross sections downstream of the inception region of free-surface aeration. The translation of the phase-detection probe in the direction normal of the invert slope was made with a Mitutoyo™ digital scale unit (accuracy ±0.025 mm).

The air-water flow signals were post-processed using a single threshold technique set at 50% of the air-water voltage (Cartellier and Achard 1991, Toombes 2002). The time-averaged void fraction C equaled the average time spent by the needle in air relative to the total sampling time. The bubble count rate F was the average number of detected particles per unit time. The air-water interfacial velocity V was derived from a cross-correlation technique, based upon the time lag corresponding to the maximum cross-correlation coefficient between leading and trailing needle signals (Serizawa et al. 1975, Cain and Wood 1981). The interfacial turbulence intensity was deduced from the broadening of the cross-correlation function relative to the auto-correlation function (Kipphan 1977, Chanson and Toombes 2002).

In the three-dimensional model of the Hinze Dam stepped spillway, the air-water flow measurements were conducted for three different water discharges, corresponding to three series of prototype observations undertaken during the March 2021 floods (Table 1). The corresponding ratios of critical flow depth to vertical step height were d_c/h = 1.0, 1.33 and 1.58, with $d_c = (q^2/g)^{1/3}$, q the unit discharge, and g the gravity constant. The three flow rates corresponded to some skimming flow conditions and are listed in Table 1.

Table 1. Froude similar experiments of laboratory and prototype observations of self-aeration at the Hinze Dam stepped spillway

Reference	θ (°)	B (m)	h (m)	q (m^2/s)	d_c/h	Comment
Laboratory	51.3	0.985	0.10	0.0954 0.1523 0.1959	0.98 1.33 1.58	University of Queensland
Hinze Dam spillway	51.3	12.25	1.5	5.86 9.05 11.4	1.01 1.35 1.58	27 March 2021 23 March 2021 24 March 2021

Figure 2. Hinze dam stepped spillway (Australia) in 2021, h = 1.5 m, 1V:0.8H slope - From left to right: d_c/h = 1.0 (27 March 2021), shutter speed: 1/2,000s; d_c/h = 1.35 (23 March 2021), shutter speed: 1/1,000s; d_c/h = 1.58 (24 March 2021), shutter speed: 1/2,000s.

Figure 3. Laboratory experiments at the University of Queensland, h = 0.10 m, 1V:0.8H slope - From left to right: d_c/h = 0.98, 1.33 and 1.58 - Step edge numbering shown in the left photograph.

3. Air-Water Flow Features

3.1. Flow Patterns

Visual observations were conducted for unit discharges between 0.009 m^2/s and 0.195 m^2/s in the laboratory. At low flow rates, the water flowed down the stepped spillway model as a series of free-falling nappes without hydraulic jump: i.e. a nappe flow regime NA3 observed for dimensionless discharges $d_c/h < 0.45$. For a range of intermediate flow rates, i.e. $0.45 < d_c/h < 0.9$, the stepped chute flow was highly turbulent, with very strong splash and intense spray, i.e. a transition flow regime. For large discharges, corresponding to dimensionless discharges $d_c/h > 0.9$, the flow skimmed over the pseudo-bottom formed by the step edges and the mainstream was about parallel to the pseudo-invert: i.e., a skimming flow regime SK3 (Fig. 3).

In skimming flow conditions typical to large flood flows, a turbulent boundary layer formed along the staircase invert downstream of the spillway crest, and the free surface appearance varied longitudinally. Once the outer edge of the developing boundary layer interacted with the free-surface, the turbulent Reynolds stresses acting in the vicinity of the water surface overcame the combined effects of surface tension and buoyancy, leading to self-aeration (Hino 1961,

Ervine and Falvey 1987, Zabaleta et al. 2020). Downstream of the inception region, the skimming flow was self-aerated and the velocity distributions were fully-developed. In the laboratory model, a close inspection of the recirculating eddies in the step cavities suggested some irregular ejections of fluid out of the cavity into the main flow, combined with some replacement of cavity fluid near the step edge. The visual and photographic observations highlighted a high degree of main flow-cavity interactions, previously discussed by Rajaratnam (1990), Matos et al. (2001) and Chanson et al. (2002).

A systematic visual comparison between prototype and model flows was undertaken by the authors. Qualitatively, the laboratory flows presented a similar appearance to the prototype overflow events. One may compare Figures 2 and 3, with a geometric scaling ratio between prototype and laboratory model of 15:1 and a chute aspect ratio B/h equals to 8.2 and 9.85 in the prototype and model respectively, with B the chute breadth. There were however a few key differences between laboratory and prototype observations, namely (1) the extreme brightness of the air-water flow in the prototype, (2) the intense nature of air-water turbulence in the self-aerated flow region of the prototype spillway, and (3) the dark brown colour of the prototype overflow upstream of the inception region. The first point was qualitatively and quantitatively documented through the exposure and white balance settings of the dSLR cameras. The brightness of the 'white waters' at the Hinze Dam spillway generated high to very-high light values (LVs), even during overcast and heavy rain episodes, that were difficult to predict and could change very rapidly with atmospheric conditions. The second point hinted a very dynamic air entrainment process in the prototype, combined with energetic bubble-turbulence two-way coupling. The finding implied that the air bubble diffusion process in laboratory might not be in similitude with that in large prototype spillways, as discussed by Chanson (1997) and Zhang and Chanson (2017). The last and third point reflected upon the sediment-laden inflow at the prototype spillway that is a common feature in prototype hydraulic structures.

3.2. Inception Region of Free-Surface Aeration

On a steep spillway, the onset of free-surface aeration is a very dynamic transient process in prototypes (Chanson 2013). Several studies emphasised the role of longitudinal vortices developing during the rapid flow acceleration at the spillway crest and from the first step edge (Levi 1965, Toro et al. 2017, Chanson 2022b). At the Hinze Dam, the location of the inception region of free-surface aeration was constantly fluctuating about a mean location. At a given instant, the inception point was not a straight line, but rather a surface plane with some transient pattern, called herein the inception region. In both prototype and laboratory spillways, the data indicated an increasing distance of the inception region from the crest with increasing flow rate. Both prototype and model data are presented in Figure 4, with the dimensionless location of and water depth at the inception region as functions of the dimensionless Froude number F_* defined in terms of the step roughness height:

$$F_* = q / \sqrt{g \times \sin\theta \times (h \times \cos\theta)^3} \quad (1)$$

where g is the gravity acceleration, and θ is the angle between the pseudo-invert and the horizontal. In Figure 4, both prototype and laboratory data sets are compared to a semi-theoretical solution of the developing boundary layer (Chanson 1994,1995). The present data were in agreement with the literature, although the data sets indicated a shorter flow development region than predicted by the theoretical solution. In spite of some differences among the stepped spillway data sets, one must emphasise the good accuracy of the prototype data set at Hinze Dam, and a difference in crest shape between prototype and simplified laboratory model.

4. Air-Water Flow Characteristics

Downstream of the inception region, the air-water flow properties were recorded at all step edges. In the direction y normal to the main stream, the measurements were obtained above the pseudo-bottom formed by the step edges up to the upper spray area. Typical results are presented in Figures 5, 6, 7 and 8, where Y_{90} is the characteristic distance where the sir concentration equal 90%, V_{90} is the characteristics air-water velocity at $y = Y_{90}$, F_{max} is the maximum bubble frequency in the section, and d_c and V_c are the critical flow depth and velocity respectively.

The air concentration profiles followed an inverted S-shape, illustrated in Figure 5A. The air concentration distributions compared favourably to the advective diffusion theoretical model:

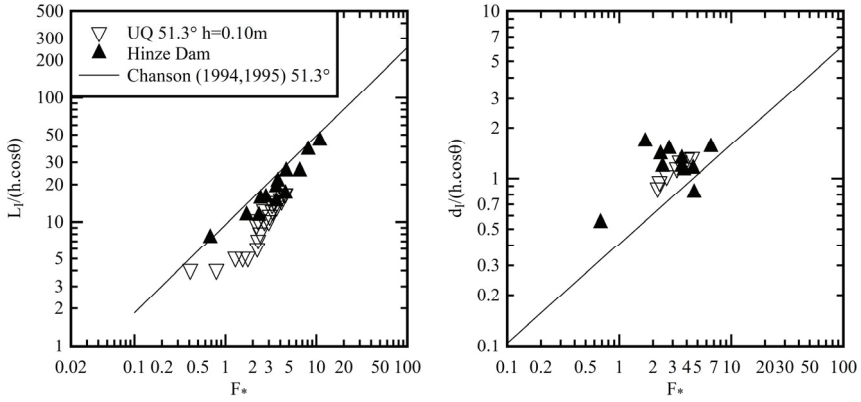

Figure 4. Inception of free-surface aeration in steep stepped spillway: comparison between Hinze Dam prototype data, 15:1 physical model and semi-analytical expressions of the turbulent boundary layer development (Chanson 1994,1995) - Same legend for both graphs.

$$C = 1 - \tanh^2\left(K - \frac{y'}{2 \times D_o} + \frac{\left(y' - 1/3\right)^3}{3 \times D_o}\right) \qquad 0 < y' < 1 \quad (2)$$

$$D' = \frac{D_o}{1 - 2 \times \left(y' - 1/3\right)^2} \qquad 0 < y' < 1 \quad (3)$$

with $y' = y/Y_{90}$, D' the dimensionless turbulent diffusivity and D_o a function of the depth-averaged air concentration C_{mean} (Chanson and Toombes 2002). The air concentration results highlighted a strong flow aeration and air-water turbulent mix of the skimming flow, with increasing aeration with increasing distance downstream of the inception region of free-surface aeration, illustrated by the increased slope of the data seen in Figure 5A. At the downstream end of the steep stepped chute, the depth-averaged air concentration C_{mean} reached about 40% for all three discharges.

The interfacial velocity data presented continuous air-water velocity profiles up to 95% to 99% of air concentration. The data showed a power law for void fractions less than 90% and an uniform profile above:

$$\frac{V}{V_{90}} = y'^{1/N} \qquad 0 < y' < 1 \quad (4)$$

$$\frac{V}{V_{90}} = 1 \qquad y' > 1 \quad (5)$$

This is illustrated in Figure 5B. In the present study, the inverse of the power law exponent N varied between 3.5 and 6, a result close to early steep stepped spillway data sets (Matos 1999, Boes 2000) and in contrast to data sets on embankment dam stepped spillway models where N varied between 7 and 12 (Gonzalez 2005, Bung 2009). Such difference in velocity distribution shape was related to different step cavity shapes, different step cavity recirculation processes and in turn different momentum exchange mechanism between the free-stream and cavity. The longitudinal variation of characteristic air-water velocity data V_{90} highlighted the air-water flow acceleration down the steep chute. The trend is presented in Figure 6, in which the present air-water flow data are compared with clear-water surface velocity data V_s measured at the Hinze Dam spillway (Chanson 2022b), a theoretical solution of the Bernoulli principle (Chanson 2001, pp. 340-341) and laboratory data (Amador 2005, Zhang 2017). The overall longitudinal trend is fascinating, with the complementary nature of prototype data, theoretical estimates and laboratory data sets. The

results (Fig. 6) further showed that the effects of boundary resistance were nil on the free-surface velocity in the non-aerated developing flow region (Fig. 6). Downstream of the inception region, on another hand, the surface velocity was smaller than ideal fluid flow estimates because of the effects of flow resistance and form drag caused by the steps.

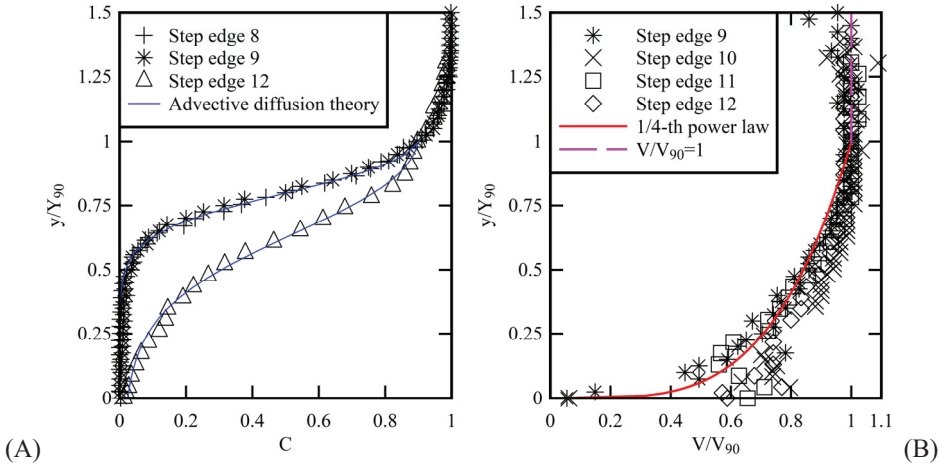

Figure 5. Dimensionless distributions of air concentration C and air-water velocity V in steep stepped spillway flow. (A) Comparison between physical model data ($d_c/h = 1.58$) and advective diffusion equation. (B) Comparison between physical model data ($d_c/h = 1.58$) and 1/4th power law.

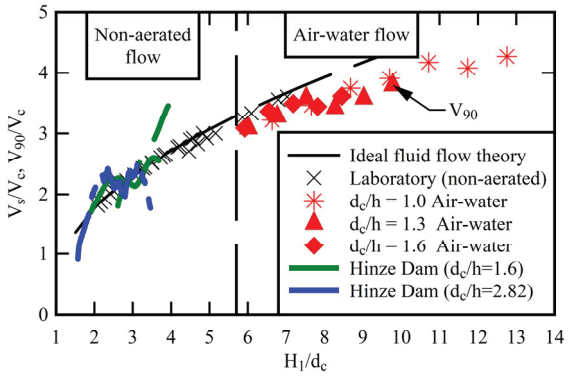

Figure 6. Dimensional longitudinal distribution of surface velocities in steep stepped spillway flow: clear-water surface velocity V_s upstream of inception region (Hinze Dam, Theory, Laboratory) and characteristic air-water velocity V_{90} (Laboratory data).

The fragmentation of the air-water flow was quantified by the bubble frequency (Fig. 7). At each step edge, the bubble frequency profile presented a marked maximum F_{max}. The relationship between bubble frequency and air concentration presented a pseudo-parabolic shape, although it was biased close to the invert under the influence of large-scale coherent structures (Fig. 7A) and reaching a maximum for void fraction between 0.35 and 0.5 (Toombes and Chanson 2008). All the data indicated an increasing maximum bubble frequency with increasing longitudinal distance (Fig. 7B) and the data did not reach an asymptotic value. The result was an important finding because it demonstrated that the air-water flow structure and the bubble-turbulence interactions evolved along the chute and did not reach any form of 'equilibrium'. This longitudinal pattern might have some implication in terms of up-scaling and model-prototype compliance.

Typical distributions of interfacial turbulence intensity are shown in Figure 8A. The profiles of turbulence intensity Tu exhibited a relatively high turbulence level across the entire air-water column, i.e. $0 < y' < 1$, typically larger than monophase flow values, e.g. Ohtsu and Yasuda (1997), Amador (2005). Although large, the current values of turbulence intensity were of the similar order of magnitude as data in wake flows between rocks and separated flows past cavities. At each step edge and for all flow rates, the relationship between bubble frequency and turbulence intensity presented a monotonic increase in turbulence intensity with increasing bubble frequency:

$$Tu - Tu_{mono} \propto F^M \qquad 0 < y' < 1 \quad (6)$$

with Tu_{mono} a typical monophase flow turbulence level on macro-roughness. Immediately downstream of the inception region, all the data suggested $M < 1$. Further downstream, the results implied $M > 1$ (Fig. 8B). The strong correlation between turbulence level and bubble frequency was linked to the quasi-parabolic relationship between bubble frequency and air concentration, and to the bubble/droplet breakup processes resulting from turbulent interactions with eddies of similar length scales as the particle (Zhang and Chanson 2016). Zhang and Chanson (2019) further demonstrated that the void fraction spectra is closely related to the air-water flow composition and fragmentation.

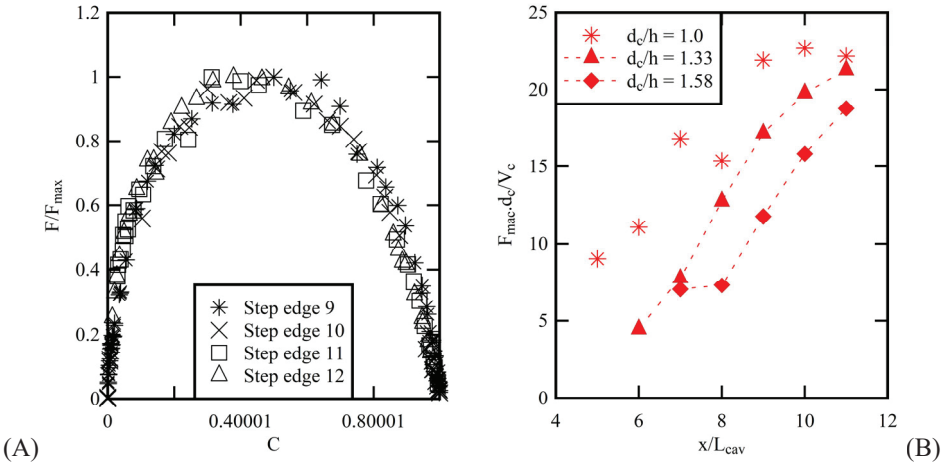

Figure 7. Flow fragmentation and bubble frequency in air-water flows on steep stepped spillway. (A) Dimensionless relationships between bubble frequency F and air concentration C for $d_c/h = 1.58$. (B) Dimensionless longitudinal distributions of maximum bubble frequency F_{max}.

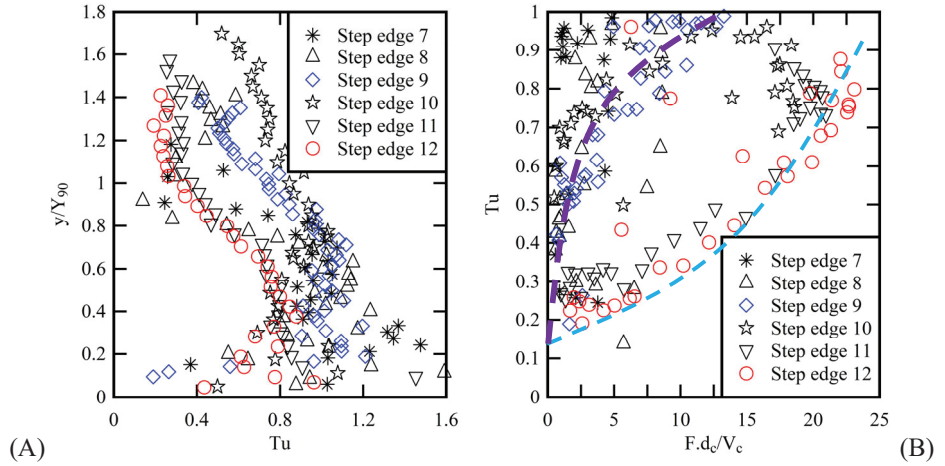

Figure 8. Dimensionless distributions of air-water turbulence intensity Tu in steep stepped spillway flow. (A) Physical model data for $d_c/h = 1.33$. (B) Dimensionless relationship between turbulence intensity and bubble frequency.

5. Discussion

In the skimming flows, the dissipation of kinetic energy was primarily a form drag process driven by the recirculation motion in the step cavities (Rajaratnam 1990, Chanson et al. 2002). In the present study, the rate of energy dissipation

was estimated, taking into account the air-water flow properties inclusive of the air-water pressure and velocity correction coefficients. That is, the total head in the air-water flows along the chute was calculated as:

$$H = \frac{\int_A \rho \times (1-C) \times V \times \left(\frac{P}{\rho \times (1-C)} + g \times z + \frac{V^2}{2} \right) \times dA}{\rho \times g \times V_{mean} \times A} \quad (7)$$

with z the vertical elevation, P the pressure and V_{mean} the cross-section averaged velocity. The rate of energy dissipation was in turn estimated as

$$\frac{\Delta H}{H_1} = \frac{H_1 - \left(\Lambda \times d \times \cos\theta + z_o + \alpha \times \frac{V_{mean}^{\ 2}}{2 \times g} \right)}{H_1} \quad (8)$$

with H_1 the upstream total head, d the equivalent clear-water depth, z_o the bed elevation, and α and Λ some air-water kinetic energy and pressure correction coefficients respectively (Chanson and Arosquipa Nina 2024). At the downstream end of stepped chute, the rate of energy dissipation $\Delta H/H_1$ ranged from 0.43 to 0.46 (Fig. 9). For a similar chute slope, chute length and unit discharge range, a smooth-invert chute would be non-aerated, and experimental data yielded a rate of energy dissipation between 0.1 and 0.2 (Halbronn 1951) (Fig. 9). Simply, the stepped spillway dissipated 2.5 to 4 times more kinetic energy than a comparable smooth chute for the same range of unit discharges.

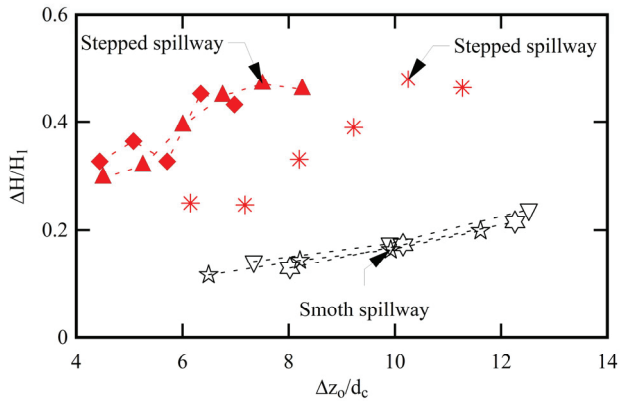

Figure 9. Dimensionless rate of energy dissipation $\Delta H/H_1$ on steep stepped spillway and comparison with steep smooth spillway data (Halbronn 1951). Same legend as Figures 6 and 7B.

6. Conclusion

The hydraulics of self-aerated flows on a steep stepped spillway was investigated based upon some composite modelling (Mark II) combining field observations and physical measurements. The spillway slope was 1V:0.8H typical of modern concrete gravity dam designs. The thrust of this study was to deliver some robust estimates of the self-aeration and rate of energy dissipation based upon detailed observations at the Hinze Dam spillway and in a 15:1 three-dimensional physical model. The upstream flow motion was accelerated and non-aerated in the skimming flows. Downstream of the inception region, some strong air entrainment and intense turbulence was recorded in the physical model. The observations were consistent with the prototype observations for Froude-similar flow conditions.

In the air-water flow region, detailed air-water flow measurements demonstrated that the air concentration distributions compared well with a theoretical model. The relationship between void fraction and bubble count rate presented a quasi-parabolic shape skewed towards the invert. The velocity profiles followed a power law, with an exponent typical of steep stepped spillways. High turbulence levels were recorded, evidences of complicated bubble-turbulence interactions and two-way coupling. The rate of energy dissipation was carefully estimated based upon detailed data sets, showing a massive increase in rate of energy dissipation along the steep stepped spillway compared to smooth-invert spillway flows, for a similar chute length and unit discharge range.

All in all, the present hybrid modelling Mark II approach combined physical and field measurements, and delivered some robust estimates directly relevant to practicing engineers. Despite a number of intrinsic challenges, this represents the ultimate methodology to obtain un-biased data sets for the proper validation of successful hydraulic designs and of both experimental and computational modelling.

7. ACKNOWLEDGEMENTS

The authors acknowledge the technical assistance of Jason Van Der Gevel and Stewart Matthews. The financial support through the School of Civil Engineering at the University of Queensland is acknowledged. In line with recommendations of the Office of the Commonwealth Ombudsman (Australia) and Committee on Publication Ethics (COPE), Hubert Chanson declares a conflict of interest with Stefan Felder (UNSW, Sydney) and Matthias Kramer (UNSW, Canberra).

8. REFERENCES

Amador, A.T. (2005). "Comportamiento Hidraulico de los Aliviaderos Escalonados en Presas de Hormigon Compactado." *Ph.D. thesis*, Univ. Polytech. of Catalunya, Barcelona, Spain, 204 pages.

Chanson, H., and Arosquipa Nina, Y. (2024). "Momentum and energy considerations in self-aerated free-surface flows." *Environmental Fluid Mechanics*, Vol. 24 (DOI: 10.1007/s10652-024-09978-w) (in Print).

Boes, R.M. (2000). "Zweiphasenströmung und Energieumsetzung an Grosskaskaden." *Ph.D. thesis*, VAW-ETH, Zürich, Switzerland (in German)

Boes, R.M., and Hager, W.H. (2003). "Hydraulic Design of Stepped Spillways." *Jl of Hydraulic Engineering*, Vol. 129, No. 9, pp. 671-679.

Bombardelli, F.A. (2012). "Computational multi-phase fluid dynamics to address flows past hydraulic structures." *Proc. 4th IAHR International Symposium on Hydraulic Structures ISHS2012*, APRH – Associação Portuguesa dos Recursos Hídricos, J. Matos, S. Pagliara, I. Meireles Editors, Keynote lecture, 19 pages.

Bung, D.B. (2009). "Zur selbstbelüfteten Gerinnenströmung auf Kaskaden mit gemässigter Neigung." *Ph.D. thesis*, University of Wuppertal, LuFG Wasserwirtschaft and Wasserbau, Germany, 292 pages (in German).

Cain, P., and Wood, I.R. (1981). "Instrumentation for Aerated Flow on Spillways." *Jl of Hydraulic Division*, Vol. 107, HY11, Nov., pp. 1407-1424.

Cartellier, A., and Achard, J.L. (1991). "Local Phase Detection Probes in Fluid/Fluid Two-Phase Flows." *Rev. Sci. Instrum.*, Vol. 62, No. 2, pp. 279-303.

Chanson, H. (1994). "Hydraulics of Skimming Flows over Stepped Channels and Spillways." *Journal of Hydraulic Res*earch, IAHR, Vol. 32, No. 3, pp. 445-460 (DOI: 10.1080/00221689409498745).

Chanson, H. (1995). "Hydraulic Design of Stepped Cascades, Channels, Weirs and Spillways." *Pergamon*, Oxford, UK, Jan., 292 pages

Chanson, H. (1997). "Air Bubble Entrainment in Free-Surface Turbulent Shear Flows." *Academic Press*, London, UK, 401 pages

Chanson, H. (2001). "The Hydraulics of Stepped Chutes and Spillways." *Balkema*, Lisse, The Netherlands, 384 pages.

Chanson, H. (2015). "Energy Dissipation in Hydraulic Structures." *IAHR Monograph*, CRC Press, Leiden, The Netherlands, 168 pages.

Chanson, H. (2022a). "Energy dissipation on stepped spillways and hydraulic challenges - Prototype and laboratory experiences." *Jl of Hydrodynamics*, Vol. 34, No. 1, pp. 52-62 (DOI: 10.1007/s42241-022-0005-8).

Chanson, H. (2022b). "Stepped Spillway Prototype Operation and Air Entrainment: Toward a Better Understanding of the Mechanisms Leading to Air Entrainment in Skimming Flows." *Journal of Hydraulic Engineering*, ASCE, Vol. 148, No. 11, Paper 05022004, 17 pages (DOI: 10.1061/(ASCE)HY.1943-7900.0002015).

Chanson, H., and Toombes, L. (2002). "Air-Water Flows down Stepped Chutes: Turbulence and Flow Structure Observations." I*nternational Jl of Multiphase Flow*, Vol. 28, No. 11, pp. 1737-1761.

Chanson, H., Yasuda, Y., and Ohtsu, I. (2002). "Flow Resistance in Skimming Flows and its Modelling." *Canadian Jl of Civil Engineering*, Vol. 29, No. 6, pp. 809-819 (DOI: 10.1139/L02-083).

Chaokitka, N., and Chanson, H. (2022). "Hydraulics of a broad-crested weir with rounded edges: physical modelling." *Proc. 30th Hydrology and Water Resources Symposium HWRS2022*, Brisbane, Australia, pp. 43-52.

Ervine, D.A., and Falvey, H.T. (1987). "Behaviour of Turbulent Water Jets in the Atmosphere and in Plunge Pools." *Proceedings of the Institution Civil Engineers, London*, Part 2, Mar. 1987, 83, pp. 295-314.

Gonzalez, C.A. (2005). "An Experimental Study of Free-Surface Aeration on Embankment Stepped Chutes." *Ph.D. thesis*, Department of Civil Engineering, The University of Queensland, Brisbane, Australia.

Halbronn, G. (1951). " Etude de la Mise en Régime des Ecoulements sur les Ouvrages à Forte Pente." *Ph.D. Thesis*, University of Grenoble, France (in French).

Hino, M. (1961). "A Theory of the Mechanism of Self-Aerated Flow on Steep Slope Channels. Applications of the Statistical Theory of Turbulence." *Technical Report C-6101*, Cent. Res. Inst. of Electric Power Ind., Japan, 42 pages.

Kipphan, H. (1977). "Bestimmung von Transportkenngrößen bei Mehrphasenströmungen mit Hilfe der Korrelationsmeßtechnik." *Chemie Ingenieur Technik*, Vol. 49, No. 9, pp. 695-707 (in German).

Levi, E. (1965). "Longitudinal Streaking in Liquid Currents." *Jl of Hydraulic Research*, Vol. 3, No. 2, pp. 25-39.

Matos, J. (1999) "Emulsionamento de ar e dissipação de energia do escoamento em descarregadores em degraus." *Ph.D. thesis*, IST, Lisbon, Portugal.

Matos, J., Yasuda, Y., and Chanson, H. (2001). "Interaction between Free-surface Aeration and Cavity Recirculation in Skimming Flows down Stepped Chutes." P*roc. 29th IAHR Biennial Congress*, Beijing, China, Theme D, Vol. 2, Tsinghua University Press, Beijing, G. Li Editor, pp. 611-617.

Matos, J., and Meireles, I. (2014). "Hydraulics of stepped weirs and dam spillways: engineering challenges, labyrinths of research." *Proc. 5th IAHR International Symposium on Hydraulic Structures (ISHS2014)*, 25-27 June 2014, Brisbane, Australia, H. Chanson and L. Toombes Editors, 30 pages (DOI: 10.14264/uql.2014.11).

Ohtsu, I., and Yasuda, Y. (1997). "Characteristics of Flow Conditions on Stepped Channels." *Proc. 27th IAHR Biennial Congress*, San Francisco, USA, Theme D, pp. 583-588.

Phillips, M., and Ridette, K. (2007). "Computational fluid dynamics models and physical hydraulic modelling - do we need both? The design of the Hinze Dam Stage 3." *Proc. 2007 NZSOLD/ANCOLD Conference*, 8 pages.

Rajaratnam, N. (1990). "Skimming Flow in Stepped Spillways." *Journal of Hydraulic Engineering*, ASCE, Vol. 116, No. 4, pp. 587-591.

Serizawa, A., Kataoka, I., and Michiyoshi, I. (1975). "Turbulence Structure of Air-Water Bubbly Flows - I. Measuring Techniques." *International Journal Multiphase Flow*, Vol. 2, No. 3, pp. 221-233.

Sorensen, R.M. (1985). "Stepped Spillway Hydraulic Model Investigation." *Journal of Hydraulic Engineering*, ASCE, Vol. 111, No. 12, pp. 1461-1472.

Toombes, L. (2002). "Experimental Study of Air-Water Flow Properties on Low-Gradient Stepped Cascades." *Ph.D. thesis*, Dept of Civil Engineering, The University of Queensland, Brisbane, Australia.

Toombes, L., and Chanson, H. (2008). "Interfacial Aeration and Bubble Count Rate Distributions in a Supercritical Flow Past a Backward-Facing Step." *International Journal of Multiphase Flow*, Vol. 34, No. 5, pp. 427-436.

Toro, J.P., Bombardelli, F.A., and Paik, J. (2017). "Detached Eddy Simulation of the Nonaerated Skimming Flow over a Stepped Spillway." *Journal of Hydraulic Engineering*, ASCE, Vol. 143, No. 9, Paper 04017032, 14 pages.

Zabaleta, F., and Bombardelli, F.A. (2020). "Eddy-resolving Simulation of Flows over Macroroughness." *Proc. RiverFlow2020*, CRC Press, Uijttewaal et al. Editors, pp. 1293-1299.

Zhang, G. (2017). "Free-Surface Aeration, Turbulence, and Energy Dissipation on Stepped Chutes with Triangular Steps, Chamfered Steps, and Partially Blocked Step Cavities." *Ph.D. thesis*, The University of Queensland, School of Civil Engineering, 361 pages (DOI: 10.14264/uql.2017.906).

Zhang, G., and Chanson, H. (2016). "Interactions between Free-surface Aeration and Total Pressure on a Stepped Chute." *Experimental Thermal and Fluid Science*, Vol. 74, pp. 368-381 (DOI: 10.1016/j.expthermflusci.2015.12.011).

Zhang, G., and Chanson, H. (2019). "On Void Fraction and Flow Fragmentation in Two-Phase Gas-Liquid Free-Surface Flows." *Mechanics Research Communications*, Vol. 96, pp. 24-28 & Digital Appendix pp. S1-S6.